HHS Public Access

Author manuscript

Magn Reson Med. Author manuscript; available in PMC 2019 June 01.

Published in final edited form as:

Magn Reson Med. 2018 June ; 79(6): 3144–3153. doi:10.1002/mrm.26985.

Quantification of Vascular Damage in Acute Kidney Injury with Fluorine Magnetic Resonance Imaging and Spectroscopy

Jeremy K. Moore, PhD[1], **Junjie Chen, PhD**[1], **Hua Pan, PhD**[1], **Joseph P. Gaut, MD, PhD**[1,2], **Sanjay Jain, MD, PhD**[1], and **Samuel A. Wickline, MD**[1,3,4,5]

[1]Department of Medicine, Washington University School of Medicine, St. Louis, Missouri

[2]Department of Pathology and Immunology, Washington University School of Medicine, St. Louis, Missouri

[3]Department of Biomedical Engineering, Washington University, St. Louis, Missouri

[4]Department of Cardiovascular Science, University of South Florida, Tampa, Florida

[5]Department of Molecular Pharmacology and Physiology, University of South Florida, Tampa, Florida

Abstract

Purpose—To design a ^{19}F MRI/MRS approach to quantify renal vascular damage after ischemia-reperfusion injury (IRI), and the therapeutic response to anti-thrombin nanoparticles to protect kidney function.

Methods—53 rats underwent 45min of bilateral renal artery occlusion and were treated at reperfusion with either plain perfluorocarbon nanoparticles or nanoparticles functionalized with a direct thrombin-inhibitor (PPACK:phenyalanine-proline-arginine-chloromethylketone). 3hrs after reperfusion, kidneys underwent ex vivo fluorine MRI/MRS at 4.7T to quantify the extent and volume of trapped nanoparticles, as an index of vascular damage and IRI. Microscopic evaluation of structural damage and nanoparticle trapping in non-reperfused renal segments was performed. Serum creatinine was quantified serially over 7 days.

Results—The damaged renal cortico-medullary junction trapped a significant volume of nanoparticles ($p=0.04$) which correlated linearly ($r=0.64$) with the severity of kidney injury 3hrs after reperfusion. Despite global large vessel reperfusion, non-reperfusion in medullary peritubular capillaries was confirmed by MRI and microscopy, indicative of continuing hypoxia due to vascular compromise. Treatment of animals with PPACK-nanoparticles after AKI did not accelerate kidney functional recovery.

Conclusion—Quantification of IRI after AKI with ^{19}F MRI/MRS of perfluorocarbon nanoparticles objectively depicts the extent and severity of vascular injury and its linear relationship to renal dysfunction. The lack of kidney function improvement after early post-treatment thrombin-inhibition confirms the rapid onset of IRI as a consequence of vascular damage and non-reperfusion. The prolongation of medullary ischemia renders cortico-medullary

Correspondence: Samuel A Wickline, M.D., University of South Florida, 12901 Bruce B. Downs Blvd., MDC 36, Tampa, FL 33612, Office Phone: 813-396-9713, wickline@health.usf.edu.

tubular structures susceptible to continued necrosis despite restoration of large vessel flow, which suggests limitations to acute interventions after AKI designed to interdict renal tubular damage.

Keywords

Fluorine MRI; AKI; vascular damage; nanoparticles; ischemia-reperfusion injury

Introduction

Microvascular injury in acute ischemic kidney injury (AKI) is proposed to play a critical role in progression to chronic renal dysfunction and fibrosis.[1–10] A technical hurdle to mechanistic evaluation of peritubular capillary damage and assessment of novel vascularly-targeted therapeutic interventions in AKI is the lack of objective *functional* and quantitative assays for defining the severity and extent of endothelial damage that may lead to persistent perfusion deficits and capillary rarefaction after ischemia-reperfusion injury. Current image-based methods such as X-ray microangiography require iodinated contrast agents that are nephrotoxic under conditions of AKI, as is also true for magnetic resonance imaging (MRI) studies employing certain gadolinium-based contrast agents that are contraindicated at low GFR's.[11,12] We propose that further development of in vivo functional imaging approaches for quantifying vascular damage that are potentially translatable to clinical environments would be of especial interest for studying vascular causes of kidney dysfunction and for examining the efficacy of novel pharmaceutical candidates for AKI and/or chronic kidney disease.

To address these concerns, we have proposed a quantitative MRI method that employs a non-nephrotoxic, semipermeable contrast agent, perfluorocarbon-core nanoparticles (PFC NP), which has been validated to date for quantification of endothelial barrier disruption in experimental atherosclerosis and AKI.[13–15] These agents previously have been used clinically as approved blood substitutes and manifest no apparent renal toxicity.[16,17] Moreover, the abundant naturally occurring fluorine (^{19}F) in the core provides a unique and quantifiable spectral magnetic resonance spectroscopy (MRS) signature with no obscuring background signal for rapid in vivo detection by MRI/MRS on clinical MRI platforms.[18–20] Circulating semi-permeant PFC NP are too large (~200 nm) to traverse *intact* vascular barriers, but under conditions of inflammation and endothelial damage can penetrate into the interstitium through breeched vascular barriers after 60–120 min circulation in vivo, where they remain trapped for detection and quantification by routine fluorine MRI/MRS methods.[14] Importantly, PFC NP also can serve as dual purpose "theranostic" agents by carrying a variety of active pharmacological ingredients to molecularly targeted sites.[21,22]

We recently reported that rodents undergoing AKI pretreated with thrombin-targeted PFC NP loaded with anti-thrombin moieties (PPACK: phenylalanine-proline-arginine-chloromethyl ketone) experience reduced thrombin deposition, attenuated microvascular injury, and hastened recovery of renal function, which was correlated with the extent of endothelial barrier disruption as detected nondestructively by ^{19}F MRI/MRS.[15] Accordingly, these and other studies[15,23–27] implicate activated thrombin as a key pharmacological target

for preventing early vascular damage in AKI. Moreover, thrombin also may serve as a molecular imaging target for high resolution quantification of microvascular damage.[19,28]

However, rigorous validation of PFC-NP as potential theranostic agents for AKI first must address several unanswered questions of translational significance. First, the relationship between the severity of acute renal injury and magnitude of the ^{19}F signal emanating from damaged microvasculature after NP trapping in disrupted microvessels is unknown. A corollary question involves the necessity for using molecularly targeted (e.g., thrombin) versus untargeted PFC-NP to delineate microvascular damage, as we have shown previously in atherosclerotic mouse models that non-targeted nanostructures suffice for longitudinal quantification of endothelial barrier disruption.[13] Second, an evaluation of *post-injury* therapy with anti-thrombin nanoparticles is lacking. Such data would help to better understand the kinetics of thrombin's deleterious consequences and whether renal ischemia-reperfusion injury might be preventable by thrombin inhibition if applied after AKI ensues. Accordingly, we studied rats undergoing 45 minutes of bilateral renal artery occlusions that were treated after injury with PPACK PFC NP and followed serially for one week to address these questions.

Methods

Nanoparticle formulation

Perfluorocarbon nanoparticles (NP, ~200 nm) were formulated with either perfluorooctylbromide (PFOB) or perfluoro-15-crown-5-ether (CE) as previously described.[28] The use of two different emulsions in certain studies allows us to examine separately the effects and distributions of nanoparticles at two different time points in the time course of AKI: pre-AKI and post-AKI. The PFOB emulsion was composed of 20% (v/v) of PFOB (Exfluor Research Corp., USA), 2.0% (w/v) of a surfactant commixture (99.9 mole% egg yolk phosphotidylcholine (Avanti Polar Lipids) and 0.1 mole% 1,2-distearoyl-sn-glyce-ro-3-phosphoethanolamine-N-(carboxy[polyethylene glycol]-2000) (Avanti Polar Lipids)), and 1.7% (w/v) glycerin, with water comprising the balance. The PFOB emulsion contained NP with a zeta potential of −7.33 mV and a diameter of 202.3 nm. The CE emulsion was composed of 20% (v/v) of CE (Exfluor Research Corp., USA), 2.0% (w/v) of the same surfactant commixture, and 1.7% (w/v) glycerin, with water comprising the balance. The CE emulsion contained NP with a zeta potential of −0.12 mV and a diameter of 176.0 nm. For therapeutic interventions, anti-thrombin PPACK was conjugated to 1,2-distearoyl-sn-glycerol-3-phosphoethanolamine-N-(carboxy[polyethylene glycol]-2000) within the PFOB NP formulation using previously reported methods that enabled loading of ~13650 PPACK moieties per particle.[28] Rhodamine (0.1mol%) and FITC (0.6 mol%) labeled phospholipids were mixed into the PFOB and CE nanoparticle formulations respectively, to render the PFC NP fluorescent.

AKI Protocol

A total of 53 adult male Sprague Dawley rats (325–350 g) acquired from Harlan Laboratories, USA were used in these studies, and all procedures were approved by the Animal Studies Committee of Washington University in St. Louis. Animals underwent

laparotomy to produce 45 minutes of bilateral warm ischemia followed by reperfusion. Briefly, rats were anesthetized with a dose of ketamine (85 mg/Kg) and xylazine (10 mg/Kg) cocktail. A mid-line abdominal incision was then performed to expose the kidneys. Kidney ischemia was induced with the use of occlusive clips situated around the isolated renal artery. Successful cessation of renal blood flow was confirmed visually by change of the kidney color from pink to dark purple. Animal body temperature was maintained at 37°C using a small animal heating system. The occlusion was released after 45 min to restore kidney blood flow, which was confirmed by the change of kidney color to pink. The surgical wound was then closed in layers and the animal recovered and returned to the cage. Sham operated animals were prepared for the 45 min laparotomy procedure except renal arteries were not occluded. Upon euthanasia, rats were perfused with saline (0.9%) via left ventricular cannulation for 5–10 minutes at a pressure of 80–100 mgHg to wash out any circulating, non-trapped PFC NP. The left kidney was extracted and fixed in 10% formalin for 48 h followed by ^{19}F MRI. The right kidney was snap frozen and later sectioned at 8mm thickness and prepared for histological analyses.

Treatment Protocols

We first sought to examine the effect of PPACK PFC NP on renal injury when treatment is given *after* AKI has developed (Figure 1). Prior to renal artery occlusion, plain (non-targeted) CE NP were injected intravenously into the tail vein at 30 min before the occlusion (2mL/kg). These NP served as a ^{19}F MRI marker for assessing intrarenal *non-reperfused* regions after AKI. Then, either PPACK PFOB NP (n=9) or plain PFOB NP (n=12) were injected intravenously into the tail vein at the time of kidney reperfusion (1mL/kg) to compare active versus placebo agent responses. A sham surgical procedure without occlusion was performed in 5 mice with CE NP injected before AKI and PFOB NP injected 45 min later, before abdominal closure. Animals were survived for 7 days prior to euthanasia and further analysis.

We next sought to study the intrarenal distributions of PFC NP as a function of timing of NP delivery (pre- vs post-AKI delivery) and the treatment (PPACK vs plain NP) to test for differences in particle access to tissue compartments. All animals were dosed with CE NP 30 min *before* AKI. For post-treatment *after* AKI, one group received plain PFOB NP (n=4) and another PPACK PFOB NP (n=5) at the time of reperfusion. A sham surgical procedure was also performed as above (n=3). Rats were euthanized 3h following AKI and kidneys excised for PFOB vs CE ^{19}F MRI/MRS.

To compare pre-AKI vs post-AKI NP trapping with MRI and the effect of the two different PFC cores on intrarenal trapping, a second group of rats received reversed dosing: plain PFOB NP *before* AKI and CE NP *after AKI* (n=12). Only plain NP were used in these experiments. To plot and evaluate the quantitative data, the pre-treatment:post-treatement ratio of 2:1 was normalized by dividing the concentration of pre-treatment nanoparticles by 2. To evaluate microscopic localization of PFC NP, another group of animals were dosed with rhodamine-labeled PFOB NP 30 min *before* AKI and FITC-labeled CE NP *after* AKI (n=3), at the time of reperfusion, for fluorescent microscopy imaging.

Serum creatinine level

Blood samples (200 μL) were collected before the procedure and at the time of euthanization for all rats. For rats in the longitudinal study, additional blood samples were collected at 6 h, 1, 2, and 3 d after AKI. Blood was centrifuged and serum creatinine concentration (mg/dL) was analyzed by AMS LIASYS 330 clinical chemistry system at the DCM Research Animal Diagnostic Laboratory, Washington University in St. Louis School of Medicine.

^{19}F MRI/MRS

All MRI experiments were carried out on a 4.7 T Varian scanner using a solenoid transmit-receive radio-frequency coil (2 cm inner diameter). The kidney was then placed in the solenoid coil and a tube of 4% trifluoroacetic acid (10 μL) was placed next to the kidney as an external standard for calibration of the kidney ^{19}F signal. The coil was first tuned to ^{1}H frequency (201.5 MHz) and a series of spin-echo images (repitition time (TR)=3 s; echo time (TE)=15 ms; number of transients (nt)=4) were acquired to locate a central slice that bisects the kidney. The coil was then turned to ^{19}F frequency (189.6 MHz) and a fluorine spectrum (TR=2 s; nt=128) from the whole kidney was acquired over 4 minutes to quantify the amount of trapped PFOB and CE NP, respectively.[29] Subsequently, ^{19}F imaging to map the intra-renal distribution of each type of NP was acquired using a fast spin-echo sequence (TR=2 s; echo spacing (ESP)=9.2 ms; echo train length (ETL)=8; nt=2048; spectral width 5760 Hz; slice thickness of 2mm). The frequency offset was changed 5371 Hz between acquiring CE and PFOB images.

Histological assessment of renal injury

Following MRI, the formalin fixed kidneys were embedded in paraffin, and sliced at 4μm thickness for routine histological staining (H&E). The severity of tubular cell damage was evaluated in blinded fashion by a pathologist with specific expertise in renal histopathology (J.G.). Microscopic examination (400×) of H&E stained slides was performed to identify and quantify features of tubular damage in the medulla, including: tubular necrosis, tubular dilation, proximal tubular brush border fragmentation, and mitotic activity. These pathologic features were expressed as a percentage of all visualized tubules within 5 randomly selected high-powered fields per slide.

Fluorescence microscopy of PFC NP

Fluorescent images of kidney cryosections were acquired to locate rhodamine-labeled PFOB NP (red) and FITC-labeled CE NP (green), respectively. For each kidney, 200× fluorescent images were acquired at 5 randomly selected positions in the medulla to determine colocalization of CE and PFOB NP.

Statistics

Serum creatinine levels over time are expressed as mean ± standard deviation (SD). Acute tubular necrosis is expressed as mean ± standard error of the mean (SEM). The concentration of trapped NP in the kidney are expressed as mean±SD. For comparisons of NP concentrations as measured by ^{19}F MRI a Kruskal-Wallis H-test was used to determine if one of the treatment groups was significantly different. Additional testing for individual

comparisons was performed with the one-tailed Mann-Whitney Test for two independent samples. P values are reported for both statistical tests.

Results

Post-AKI Effects of PPACK NP

It was previously shown that rats pretreated with PPACK NP before transient AKI improves kidney functional recovery.[15] In this study, PPACK NP were administrated after AKI and its effect on renal function was monitored over time. Figure 2A plots serum creatinine levels normalized by body weight serially through 7 d after AKI. In all animals, serum creatinine levels increased as early as 6 h after reperfusion, and peaked at 6 hours (3.78±0.95 vs 4.31±1.11, control vs treated, respectively; p=0.25). The temporal evolution of kidney function in the PPACK NP treated group did not differ significantly from that of the control (plain NP) group. The sham surgery group maintained physiological serum creatinine values throughout the recovery period. The effect of AKI and PPACK NP post-treatment on tissue architecture was evaluated by an expert renal pathologist (J.G.) in kidneys that were allowed to recover for 7 d after AKI. Blinded scoring for necrotic tubular cells (Figure 2B) was performed according to the described methodology. No significant difference (p=0.56) was identified between plain NP treatment (24%±11%) and PPACK NP treatment (20%±7%) groups at this time point, as seen in Figure 2C and D respectively. The normal kidneys from the sham procedure showed no signs of tubular necrosis or injury.

Nanoparticle Trapping Before and After AKI

To determine if differences existed in access of pre- versus post-treatment PFC NP regarding either localization or concentration, we pre-treated a group of rats with PFOB NP, followed by AKI, and then post-AKI with CE NP. Animals were euthanized 3 hours after AKI and systemically perfused with saline to wash out circulating NP, leaving NP trapped in non-reperfused vascular territories (either extravasated or in microthrombi) for ^{19}F detection. ^{19}F MRI was used to quantitatively map the trapped PFOB and CE NP, as described previously.[13] Figure 3A illustrates an overlay of the ^{19}F images atop a ^{1}H kidney image. In Figure 3B, a ^{1}H image of an injured kidney, the inner medulla of the injured kidney exhibited an abnormally low ^{1}H signal (shorter T_2^* times) as a likely consequence of blood accumulation in the microvasculature.[30,31] Correspondingly, the ^{19}F image of both pre-treated PFOB NP (Figure 3C, red) and post-treated CE NP (Figure 3D, green) showed trapping of both types of NP (Figure 3A, combined into yellow) in the inner medulla of the injured kidneys.

To depict the role of molecular targeting of PFC NP in medullary trapping, Figure 3E demonstrates that the damaged kidneys trap a significant amount of NP by 3 h after AKI as compared to a sham group. Moreoever, trapped PFC NP are present in non-reperfused regions at 7 days. The sham surgery group exhibited significantly less ^{19}F signal at 3 hours after reperfusion than did the other two groups (p=0.04 by Kruskal-Wallis test; [NP] sham=0.69±0.48 μL/g; [NP] control=3.34±1.13 μL/g; [NP] PPACK=4.64±3.20 μL/g), but by 7 days no difference among groups was noted (p=0.09; [NP] sham=0.72±0.21 μL/g; [NP] control=2.98±3.47 μL/g; [NP] PPACK=1.73±1.08 μL/g). Additional statistical analysis with a one-tailed Mann-Whitney test for two independent variables confirmed that the control and

PPACK groups were significantly different ($p<0.03$) than the sham surgery group. The sham group exhibited a small amount of NP that were not washed out of the kidney. These NP were evenly dispersed at low levels throughout the kidney as seen by ^{19}F MRI (not shown) and did not change in quantity from 3 h to 7 days (Figure 3E).

Accumulation of blood (hemorrhage) was observed by light microscopy in the AKI kidney image in Figure 4. For the sham surgery procedure, no visual evidence of blood was observed by light microscopy. This hemorrhagic region appears as the low ^{1}H MRI signal in Figure 3B and correlated NP trapping is illustrated in Figure 3C and D.

Figure 5 correlates the quantity of trapped pre-treated NP versus that of trapped post-treated NP at 3 h after AKI. Here one group of rats was pre-treated with CE NP and post-treated with PFOB NP (filled circles). A second group of rats (open squares) had the regimens reversed by pre-treating with PFOB NP and then post-treating with CE NP. These data illustrate linear correlations in both cases ($r=0.99$ for CE pre-treatment and $r=0.96$ for PFOB pre-treatment). We should note however, that the slope for the PFOB pretreated regimen (2.04) exceeds that for the CE pretreatment regimen (1.22), indicating that when PFOB is given first, there is relatively more post treatment CE left after 3 hours of reperfusion (i.e., a greater ratio/slope: squares) than if PFOB is given last (circles). This may be explained in part by the known faster tissue clearance rate for PFOB (tissue half-life of 4 days)[17,32–34] than for CE (~100 days)[32–34]. This evidence for NP clearance would be qualitatively consistent with the apparent clearance of pre-treatment CE NP noted in Figure 3E over the 7 day interval.

Kidney Dysfunction Reflects the Extent of Vascular Damage

We have shown previously that ^{19}F NP trapping quantitatively reflects microvascular damage in mouse models of atherosclerosis.[13,14] Figure 6 illustrates that the measured quantity of trapped NP in whole kidneys also correlates with kidney function in both pre-treatment and post-treatment NP regimens ($r=0.64$ for both treatments). The overall quantity of trapped NP in injured kidneys was determined by ex vivo ^{19}F MRS and normalized by the weight of kidney. The NP concentration is plotted for both the pre- and post-injury injections, which are compensated for the 2:1::pre-treament:post-treatment administered dose ratio that was used to adjust for expected differences in signal intensity between PFOB and CE. Kidney function was measured as a change in serum creatinine concentration from baseline to the level observed at the time of euthanasia, 3 h after reperfusion.

Localization of Pre- and Post-treatment NP Trapping in Kidney Microvasculature Structures

Although the trapping of therapeutically inefficacious post-treated NP in the inner medulla appears comparable to that of pre-treated NP by low resolution MRI/MRS criteria, Figure 7 indicates that nanoparticles injected at two different time points are not entirely colocalized. Pre-treatment particles (PFOB) labeled with rhodamine (red) and post-treatment particles (CE) labeled with FITC (green) sometimes colocalize (yellow-orange color), but are also observed situated in distinct regions (either pure red or green). Sham surgical procedures resulted in no detectable fluorescent signal for either NP.

Discussion

The ability to quantitatively image vascular damage that occurs during AKI and through the extension phase can provide important pathophysiological insights into AKI.[15,35] Toward this goal, for example, Kramman et al[4] recently extended the initial work of Advani et al[36] to implement a fluorescence microangiographic assay using perfusable micron-sized fluorescent beads coupled with algorithmic quantification of microscopic changes in renal peritubular capillaries (e.g., number density and caliber). They demonstrated a clear relationship between early renal injury (24 hours after AKI) measured by elevated BUN (blood urea nitrogen), and later (8 week) capillary damage, suggesting that the initial ischemic insult to the microvasculature itself is a critical determinant of impaired renal function.

The current study proposes an alternative and potentially in vivo methodology to evaluate vascular damage in AKI that utilizes quantitative fluorine (^{19}F) MRI readouts of molecular signatures emanating from perfluorocarbon nanoparticles perfusing the kidney in vivo as a new option for imaging ischemic endothelial damage. Additionally, we sought to evaluate the use of the same nanoparticles when functionalized to contain thrombin inhibitors as a novel theranostic approach for treating and monitoring AKI. We observed that the quantity of NP trapped in kidneys after AKI was linearly correlated with the severity of kidney injury as measured by ^{19}F MRI, which suggests that this technique could be useful for noninvasive delineation of renal vascular damage (i.e., non-reperfusion). Local non-reperfusion in peritubular capillaries was apparent even after global reperfusion, which confirms that severe and persistent vascular damage occurs early during AKI and ischemia persists as a likely cause of sustained regional hypoxia and tubular cell death. However, kidney functional recovery was not improved by post-AKI treatment with thrombin-inhibiting nanoparticles, despite an earlier report from our group that *pretreatment* with the same therapeutic nanoparticle was effective at preventing vascular damage and restoring nutritive perfusion to an extent.[15]

It has been proposed the “extension phase of ischemic injury” plays a critical role in AKI,[1] manifested in part by persistent regional intra-renal non-reperfusion after the restoration of renal blood flow following transient ischemia.[37] Several factors could contribute to regional non-reperfusion, including (1) swelling of ischemically injured endothelial cells resulting in reduced capillary lumen size, which may block the passage of red blood cells; or even death and endothelial cell sloughing plugging capillary lumens; (2) ischemia induced inflammatory responses that recruit inflammatory cells producing various factors such as superoxides that potentiate ongoing damage; (3) an activated clotting cascade leading to thrombosis and vessel plugging. In this study, ^{19}F MRI results revealed that NP delivered either before or after AKI was induced could be observed in the cortico-medullary (CM) junction (Figure 3) where hemorrhage was observed as a direct consequence of vascular damage (see Figure 4 and also note low T1w signal on T1w images in Figure 3B). Minimal nanoparticle trapping was observed in the cortex where the transient damage that occurs is readily reversed upon kidney reperfusion.[1] Thus, the data indicate that NP trapping within the renal medulla is consistent regardless of the time point chosen for investigation. The MRI data indicate that the cortical regions are indeed better reperfused after AKI than are

the CM junction regions where sustained non-reperfusion is concentrated in the peritubular capillaries. In this region, severe hypoxia coupled with high energetic demands lead to disruption of vascular integrity (hemorrhage) and severe acute tubular damage. Accordingly, successful reperfusion of the cortex is not sufficient to restore renal function in this model and the sustained non-reperfusion at the CM junction is responsible for renal dysfunction that recovers only slowly over time. Despite the apparent delivery of thrombin-targeted nanoparticles to similar medullary regions whether administered before or after AKI, the lack of treatment efficacy (Figure 2A) suggest that thrombin's deleterious actions are too immediate for intervention by post-treatment therapeutics even though thrombin, clearly, is a valid target. Pre- and post-treatment strategies appear to differ significantly in NP delivery kinetics as evidenced by differences in microscopic trapping sites (Figure 7) and quantities (Figure 5). The microscopic evidence of non-colocalized nanoparticle trapping suggests that smaller nutritive vessels may not be accessible after AKI, even if larger vessels admit nanoparticles to the same general areas. This rapid onset of non-reperfusion may be one cause for widespread clinical failure of most therapies to interdict AKI when administered after injury.

Both PPACK –targeted and non-targeted NP are trapped to the same extent (Figure 3E), indicating that molecular targeting of thrombin is not affecting the local deposition of the nanoparticles and that it is a passive event not requiring binding to a specific molecular tether to be retained in the injured medulla. The linear relationship between pre- and post-treatment trapping, seen in Figure 5, suggests that passive intra-renal trapping evenly distributes the NP regardless of the time of treatment or the type of NP used for treatment. Altogether this indicates that ^{19}F MRI of PFC NP is able to depict the regional severity of medullary damage across a range of ischemic insults.

The presence of regional non-reperfusion after AKI might suggest that anti-thrombotic therapy could benefit kidney recovery by preventing non-reperfusion. In a previous study we showed that pre-AKI treatment with anti-thrombin PPACK NP was effective in targeting and inhibiting thrombin activity as well as improving kidney functional recovery after AKI.[15] Other reports also have confirmed that anti-thrombin therapies with NP are able to improve kidney recovery.[23–27] For example, Sharfuddin in the Molitoris group[23] used recombinant thrombomodulin, a thrombin cofactor in the anticoagulation pathway of activated protein C, to improve kidney function in both pre-treatment and post-treatment regimens. In this study, the post-treatment effect of PPACK NP revealed no significant difference in renal recovery following AKI. The reason for the difference in outcomes between the two post-AKI treatment strategies may relate to the timing of the therapies, in our case delivered within a few minutes after restoration of flow and in the Molitoris work 2 hours after reperfusion. It is possible that immediate thrombosis thwarted access of our PPACK NP to sites of injury as Enestrom et al have shown clear evidence of extensive deposition of fibrinous clots in peritubular capillaries and vasa recta small vessel obstruction as early as 5 minutes after reperfusion, peaking at 15 minutes, all of which was preventable by heparin delivered before reperfusion.[7] These thrombi gradually dissipate by lysis over the following hour, perhaps allowing better access of the thrombomodulin to sites of injury 2 hours later when occlusion was less prevalent, as contrasted with our case where much earlier delivery of PPACK NP would encounter more extensive thrombotic obstruction affording less penetration.

Regarding mechanisms of nanoparticle accumulation in nonreperfused zones, because kidney damage and nonreperfusion evolves rapidly within 15 min,[7] there is little possibility that uptake by circulating immune cells could be responsible for the observed NP trapping. Indeed, we have reported previously that no appreciable uptake of PFC NP by circulating white blood cells is notable within 30 min post-injection.[13] In the present work, the 45 min occlusion time followed by nonreperfusion leaves little chance for immune cells to deliver any substantial influx of NP.[38] The pretreatment particles are expected to be either extravasated or contained within microvascular thrombi (Figures 2 and 5), and the post treatment particles appear capable of reaching the same general locations though not into therapeutically relevant structures, as discussed above.

Our previous report of the benefit of pretreatment with thrombin inhibiting PPACK NP[15] together with the lack of efficacy of immediate post-AKI treatment in this study argues that microvascular thrombosis due to activation of thrombin is clearly a high value target for therapeutic intervention but that it occurs too rapidly either during or after ischemic injury to prevent once AKI is established. According to the careful examination of early thrombosis in AKI by Enestrom et al,[7] the actual ischemia times in AKI may be far greater than anticipated in experimental and clinical AKI based on recorded occlusion times or periods of hypoperfusion. After clot dissolution, the vasculature might be “perfusable” to an extent, yet manifest severe endothelial damage sufficient to trap PFC NP in an edematous interstitial compartment under conditions that would further compromise oxygen and nutrient flow to tubular cells well beyond the time of complete microvascular obstruction.

Previous MRI studies of AKI have utilized techniques such as the BOLD (blood oxygenation level-dependent) effect[39,40] and arterial spin labeling (ASL) to assess renal damage and abnormal perfusion.[41–43] The BOLD effect allows for a measure of renal tissue oxygen tension which reveals initial and sustained hypoxic conditions in AKI. ASL allows for measurement of regional perfusion within the kidney. We reported previously that renal perfusion can be delineated in vivo by ^{19}F MRI with PFC NP[15] and that tissue deposition of PFC NP can be quantified on clinical 3T imaging platforms.[13] An advantage of this approach is the ability to delineate quantitatively the absolute volume of the damaged and nonreperfused vascular territories according to the trapped ^{19}F signal despite apparent global reperfusion with a non renotoxic contrast agent. The quantitative results obtained with ^{19}F MRI of PFC NP suggest that NP trapping due to microvascular damage is correlated with acute kidney dysfunction and could thus serve as a potential proxy for vascular disruption if confirmed in more extensive studies.

Previous studies have examined ^{19}F MRI of PFC NP that are molecularly targeted to sites of thrombosis.[28,44] These studies indicate the potential of thrombin targeted NP to serve as theranostic agents that both inhibit and image developing thrombi with the use of specific ^{19}F MRI signatures. Although we have reported previously that thrombin-targeted nanoparticles are useful for improving kidney function after AKI when administered prior to ischemic events, here we report that thrombin-targeted NP do not enhance recovery of kidney function when administered after ischemic injury due to the rapidity of onset of the nonreperfusion condition. Nevertheless, the extent of nonreperfusion can be depicted by ^{19}F MRI, which offers a potentially noninvasive and quantifiable method for evaluating the

severity of regional renal damage after AKI. In summary, our data suggest that the ability of ^{19}F spectroscopy and imaging to depict the regional severity of barrier disruption with a quantitative metric that is directly correlated with the severity of renal injury (Figure 3 and 5) offers a non-nephrotoxic approach to assessing vascular injury and healing that accompany recovery of kidney function after AKI. Early post-AKI treatment with anti-thrombin PPACK NP did not improve kidney functional recovery likely due to poor access of agents to the obstructed microvasculature. These observations taken together suggest a cautionary message: the prolongation of regional medullary ischemia for hours beyond reperfusion renders cortico-medullary tubular structures susceptible to continued necrosis despite restoration of large vessel flow, which suggests that there may be significant limitations to acute interventions after AKI, such as thrombin inhibition, that are proposed to interdict renal tubular damage. These considerations argue for alternative therapeutic approaches that might focus more on restoring vascular integrity beyond the acute phases of ischemic kidney injury.

Acknowledgments

The authors would like to thank Lei Cai, Stacy Allen, and Hiuying Zhang for technical assistance with this work. This investigation was supported by National Institutes of Health, National Research Service Award 5-T32-HL07081-41, from the National Heart, Lung, and Blood Institute, and NIH grants HL073646 and DK102691. Dr. S. A. Wickline reports equity interest in AcuPlaq, LLC.

References

1. Basile DP, Anderson MD, Sutton TA. Pathophysiology of acute kidney injury. Comprehensive Physiology. 2012; 2(2):1303–1353. [PubMed: 23798302]
2. Sutton TA, Fisher CJ, Molitoris BA. Microvascular endothelial injury and dysfunction during ischemic acute renal failure. Kidney International. 2002; 62(5):1539–1549. [PubMed: 12371954]
3. Molitoris BA, Sutton TA. Endothelial Injury and Dysfunction: Role in the Extension Phase of Acute Renal Failure. Kidney International. 2004; 66:496–499. [PubMed: 15253696]
4. Kramann R, Tanaka M, Humphreys BD. Fluorescence Microangiography for Quantitative Assessment of Peritubular Capillary Changes after AKI in Mice. Journal of the American Society of Nephrology. 2014; 25:1924–1931. [PubMed: 24652794]
5. Maringer K, Sims-Lucas S. The multifaceted role of the renal microvasculature during acute kidney injury. Pediatric Nephrology. 2016; 31(8):1231–1240. [PubMed: 26493067]
6. Akhtar AM, Schneider JE, Chapman SJ, Jefferson A, Digby JE, Mankia K, Chen Y, Mcateer MA, Wood KJ, Choudhury RP. In Vivo quantification of vcam-1 expression in renal ischemia reperfusion injury using non-invasive magnetic resonance molecular imaging. PLoS ONE. 2010; 5(9):1–10.
7. Eneström S, Druid H, Rammer L. Fibrin deposition in the kidney in post-ischaemic renal damage. British journal of experimental pathology. 1988; 69(3):387–94. [PubMed: 3291926]
8. Yamamoto T, Tada T, Brodsky SV, Tanaka H, Noiri E, Kajiya F, Goligorsky MS. Intravital Videomicroscopy of Peritubular Capillaries in Renal Ischemia. American Journal of Renal Physiology. 2002; 282:1150–1155.
9. Verma SK, Molitoris BA. Renal Endothelial Injury and Microvascular Dysfunction in Acute Kidney Injury. Seminars in Nephrology. 2015; 35(1):96–107. [PubMed: 25795503]
10. Zafrani L, Payen D, Azoulay E, Ince C. The Microcirculation of the Septic Kidney. Seminars in Nephrology. 2015; 35(1):75–84. [PubMed: 25795501]
11. Ersoy H, Rybicki FJ. Biochemical Safety Profiles of Gadolinium-Based Extracellular Contrast Agents and Nephrogenic Systemic Fibrosis. Journal of Magnetic Resonance Imaging. 2007; 26(5): 1190–1197. [PubMed: 17969161]

12. Neuwelt EA, Hamilton BE, Varallyay CG, Rooney WR, Edelman RD, Jacobs PM, Watnick SG. Ultrasmall superparamagnetic iron oxides (USPIOs): a future alternative magnetic resonance (MR) contrast agent for patients at risk for nephrogenic systemic fibrosis (NSF)? Kidney International. 2009; 75(5):465–474. [PubMed: 18843256]
13. Palekar RU, Jallouk AP, Goette MJ, Chen J, Myerson JW, Allen JS, Akk A, Yang L, Tu Y, Miller MJ, et al. Quantifying progression and regression of thrombotic risk in experimental atherosclerosis. FASEB. 2015; 29(7):3100–3109.
14. Palekar RU, Jallouk AP, Myerson JW, Pan H, Wickline SA. Inhibition of thrombin with PPACK-nanoparticles restores disrupted endothelial barriers and attenuates thrombotic risk in experimental atherosclerosis. Arteriosclerosis, Thrombosis, and Vascular Biology. 2016; 36(3):446–455.
15. Chen J, Vemuri C, Palekar RU, Gaut JP, Goette M, Hu L, Cui G, Zhang H, Wickline SA. Antithrombin nanoparticles improve kidney reperfusion and protect kidney function after ischemia-reperfusion injury. American Journal of Physiology. Renal Physiology. 2015; 308(7): 765–773.
16. Cohn CS, Cushing MM. Oxygen Therapeutics: Perfluorocarbons and Blood Substitute Safety. Critical Care Clinics. 2009; 25(2):399–414. [PubMed: 19341916]
17. Spahn DR. Blood substitutes Artificial oxygen carriers: perfluorocarbon emulsions. Critical Care. 1999; 3(5):93–97.
18. Chen J, Lanza GM, Wickline SA. Quantitative magnetic resonance fluorine imaging: today and tomorrow. Nanomedicine and nanobiotechnology. 2010; 2(4):431–440. [PubMed: 20564465]
19. Chen J, Pan H, Lanza GM, Wickline SA. Perfluorocarbon nanoparticles for physiological and molecular imaging and therapy. Advances in chronic kidney disease. 2013; 20(6):466–478. [PubMed: 24206599]
20. Partlow KC, Chen J, Brant JA, Neubauer AM, Meyerrose TE, Creer MH, Nolta JA, Caruthers SD, Lanza GM, Wickline SA. 19F magnetic resonance imaging for stem/progenitor cell tracking with multiple unique perfluorocarbon nanobeacons. FASEB. 2007; 21(8):1647–1654.
21. Palekar RU, Jallouk AP, Lanza GM, Pan H, Wickline SA. Molecular imaging of atherosclerosis with nanoparticle-based fluorinated MRI contrast agents. Nanomedicine. 2015; 10(11):1817–1832. [PubMed: 26080701]
22. Pan D, Caruthers SD, Chen J, Winter PM, SenPan A, Schmieder AH, Wickline SA, Lanza GM. Nanomedicine strategies for molecular targets with MRI and optical imaging. Future medicinal chemistry. 2010; 2(3):471–490. [PubMed: 20485473]
23. Sharfuddin AA, Sandoval RM, Berg DT, McDougal GE, Campos SB, Phillips CL, Jones BE, Gupta A, Grinnell BW, Molitoris BA. Soluble Thrombomodulin Protects Ischemic Kidneys. Journal of the American Society of Nephrology. 2009; 20(3):524–534. [PubMed: 19176699]
24. Gottmann U, Mueller-Falcke A, Schnuelle P, Birck R, Nickeleit V, van der Woude FJ, Yard BA, Braun C. Influence of hypersulfated and low molecular weight heparins on ischemia/reperfusion: injury and allograft rejection in rat kidneys. Transplant International. 2007; 20(6):542–549. [PubMed: 17355246]
25. Ozden A, Sarioglu A, Demirkan N, Bilgihan A, Duzcan E. Antithrombin III Reduces Renal Ischemia-Reperfusion Injury in Rats. Research in Experimental Medicine. 2001; 200(3):195–203. [PubMed: 11426671]
26. Favreau F, Thuillier R, Cau J, Milin S, Manguy E, Mauco G, Zhu X, Lerman LO, Hauet T. Anti-thrombin therapy during warm ischemia and cold preservation prevents chronic kidney graft fibrosis in a DCD model. American Journal of Transplantation. 2010; 10(1):30–39. [PubMed: 19958330]
27. Ozaki T, Anas C, Maruyama S, Yamamoto T, Yasuda K, Morita Y, Ito Y, Gotoh M, Yuzawa Y, Matsuo S. Intrarenal administration of recombinant human soluble thrombomodulin ameliorates ischaemic acute renal failure. Nephrology Dialysis Transplantation. 2008; 23(1):110–119.
28. Myerson J, He L, Lanza G, Tollefsen D, Wickline SA. Thrombin-inhibiting perfluorocarbon nanoparticles provide a novel strategy for the treatment and magnetic resonance imaging of acute thrombosis. Journal of Thrombosis and Haemostasis. 2011; 9(7):1292–1300. [PubMed: 21605330]
29. Morawski AM, Winter PM, Yu X, Fuhrhop RW, Scott MJ, Hockett F, Robertson JD, Gaffney PJ, Lanza GM, Wickline SA. Quantitative “magnetic resonance immunohistochemistry” with ligand-

targeted 19F nanoparticles. Magnetic Resonance in Medicine. 2004; 52(6):1255–1262. [PubMed: 15562481]

30. Mason J, Torhorst J, Welsch J. Role of the medullary perfusion defect in the pathogenesis of ischemic renal failure. Kidney Int. 1984; 26(3):283–293. [PubMed: 6513274]
31. Yamamoto K, Wilson DR, Baumal R. Outer medullary circulatory defect in ischemic acute renal failure. The American journal of pathology. 1984; 116(2):253–261. [PubMed: 6465286]
32. Riess JG. Oxygen carriers ("blood substitutes") - Raison d'etre, chemistry, and some physiology. Chemical Reviews. 2001; 101(9):2797–2919. [PubMed: 11749396]
33. Riess JG. Reassessment of Criteria for the selection of perfluorochemicals for second-generation blood substitutes: analysis of structure/property relationships. Artificial Organs. 1984; 8(1):44–56. [PubMed: 6703926]
34. Krafft, MP., Riess, JG., Weers, JG. Submicron emulsions in drug targeting and delivery. Amsterdam: Harwood Academic; 1998. The design and engineering of oxygen-delivering fluorocarbon emulsions; p. 235
35. Wang E, Sandoval RM, Campos SB, Molitoris BA. Rapid diagnosis and quantification of acute kidney injury using fluorescent ratio-metric determination of glomerular filtration rate in the rat. American Journal of Physiology-Renal Physiology. 2010; 299(5):1048–1055.
36. Advani A, Connelly KA, Yuen DA, Zhang Y, Advani SL, Trogadis J, Kabir MG, Shachar E, Kuliszewski MA, Leong-Poi H, et al. Fluorescent microangiography is a novel and widely applicable technique for delineating the renal microvasculature. PLoS ONE. 2011; 6(10)
37. Sutton TA. Alteration of microvascular permeability in acute kidney injury. Microvasc Res. 2009; 77(1):4–7. [PubMed: 18938184]
38. Uitterdijk A, Sneep S, van Duin RW, Krabbendam-Peters I, Gorsse-Bakker C, Duncker DJ, van der Giessen WJ, van Beusekom HM. Serial measurement of hFABP and high-sensitivity troponin I post-PCI in STEMI: how fast and accurate can myocardial infarct size and no-reflow be predicted? Am J Physiol Heart Circ Physiol. 2013; 305(7):1104–1110.
39. Hu L, Chen J, Yang X, Senpan A, Allen JS, Yanaba N, Caruthers SD, Lanza GM, Hammerman MR, Wickline SA. Assessing intrarenal nonperfusion and vascular leakage in acute kidney injury with multinuclear $^{1}H/^{19}F$ MRI and perfluorocarbon nanoparticles. MRM. 2014; 71(6):2186–2196. [PubMed: 23929727]
40. Pohlmann A, Hentschel J, Fechner M, Hoff U, Bubalo G, Arakelyan K, Cantow K, Seeliger E, Flemming B, Waiczies H, et al. High temporal resolution parametric MRI monitoring of the initial ischemia/reperfusion phase in experimental acute kidney injury. PLoS ONE. 2013
41. Zimmer F, Klotz S, Hoeger S, Yard BA, Kramer BK, Schad LR, Zollner FG. Quantitative Arterial Spin Labelling Perfusion Measurements in Rat Models of Renal Transplantation and Acute Kidney Injury at 3T. Z Med Phys. 2017; 27(1):39–48. [PubMed: 27017515]
42. Hueper K, Gutberlet M, Rong S, Hartung D, Mengel M, Lu X, Haller H, Wacker F, Meler M, Gueler F. Acute kidney injury: arterial spin labeling to monitor renal perfusion impairment in mice-comparison with histopathologic results and renal function. Radiology. 2014; 270(1):117–124. [PubMed: 24023073]
43. Klotz S, Pallavi P, Tsagogiorgas C, Zimmer F, Zollner FG, Binzen U, Greffrath W, Treede R, Walter J, Harmsen MC, et al. N-octanoyl dopamine treatment exerts renoprotective properties in acute kidney injury but not in renal allograft recipients. Nephrol Dial Transplant. 2016; 31(4):564–573. [PubMed: 26454224]
44. Temme S, Grapentin C, Quast C, Jacoby C, Grandoch M, Ding Z, Owenier C, Mayenfels F, Fischer JW, Schubert R, Schrader J, Flogel U. Noninvasive imaging of early venous thrombosis by ^{19}F magnetic resonance imaging with targeted perfluorocarbon nanoemulsions. Circulation. 2015; 131:1405–1414. [PubMed: 25700177]

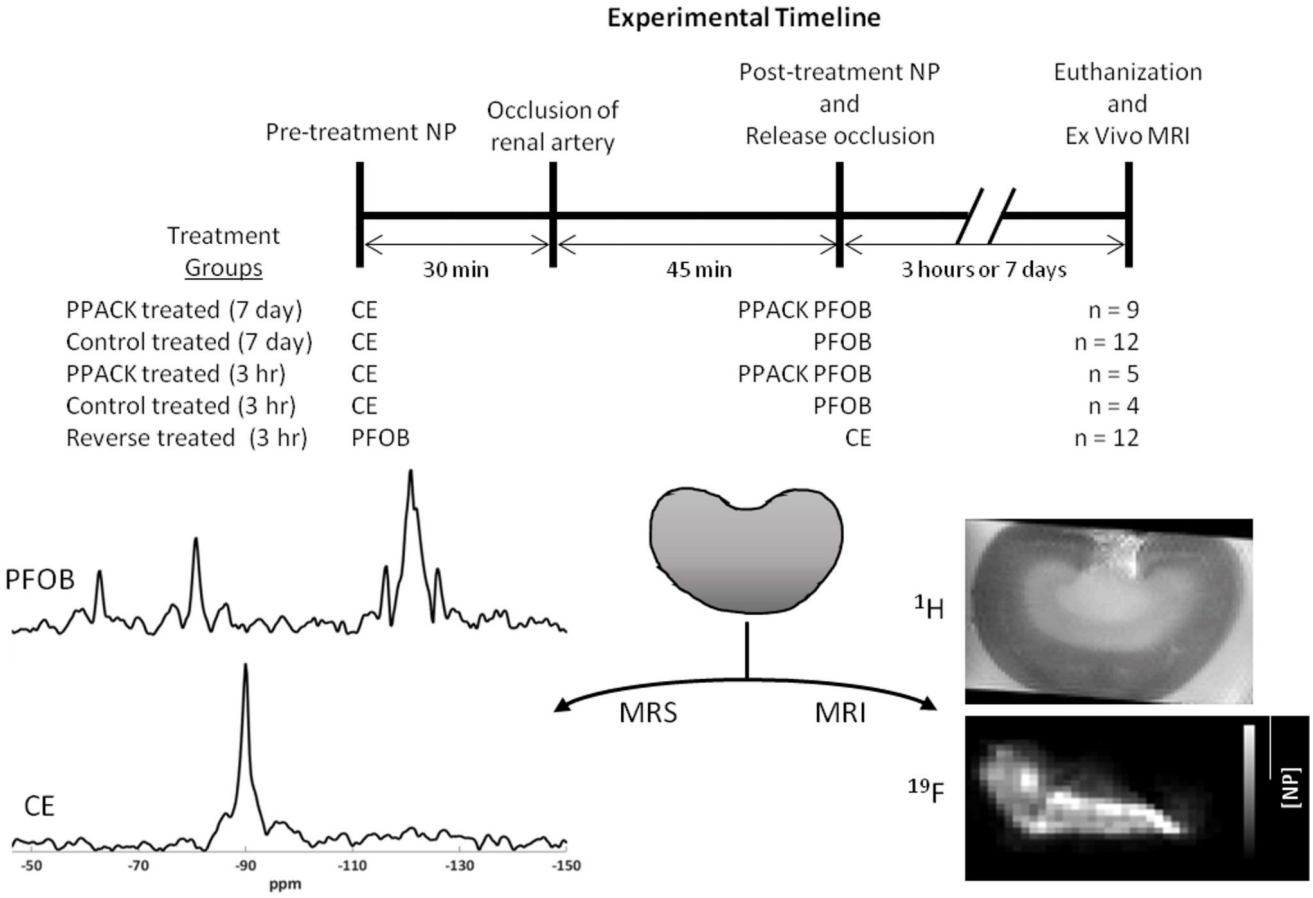

Figure 1.

The experimental timeline illustrates the timing of NP treatments, AKI, and euthanization. The treatment groups are listed with the NP used shown below the pre-treatment and post-treatment lines on the timeline. Examples of ^{19}F spectra and images that were recorded from the excised kidneys are shown.

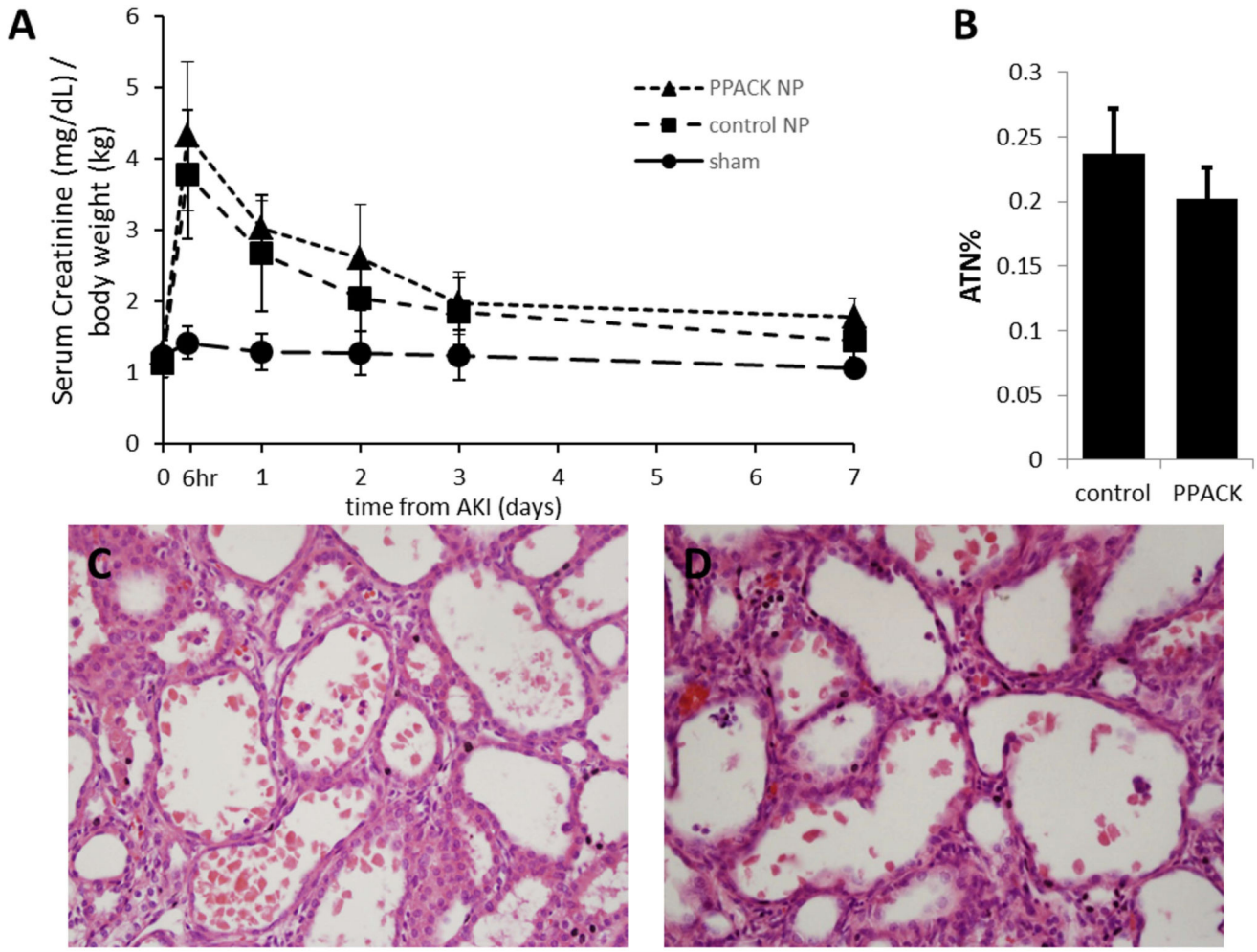

Figure 2.

PPACK NP treatment after AKI did not hasten kidney functional recovery. (A) Rats that underwent transient bilateral warm AKI (45 min) manifested an acute increase of serum creatinine levels after reperfusion. Compared to the sham group, [Cr], in both PPACK NP and plain NP treated groups peak at 6 h after reperfusion. However, no significant difference of [Cr] was observed between PPACK NP and plain NP treated groups at any time point. Data are presented as means ±SD. n=9 for PPACK NP group; n=12 for plain NP group; n=5 for Sham group. The acute tubule necrosis percent (B) indicates that the groups are comparable (p=0.56). Data are presented as means ±SEM. n=9 for PPACK NP group; n=11 for plain NP group. H&E staining is shown for a plain NP treated kidney (C) and a PPACK NP treated kidney (D). These examples indicate the lack of structural differences at the light microscopic level between the two treatment groups, PPACK and control.

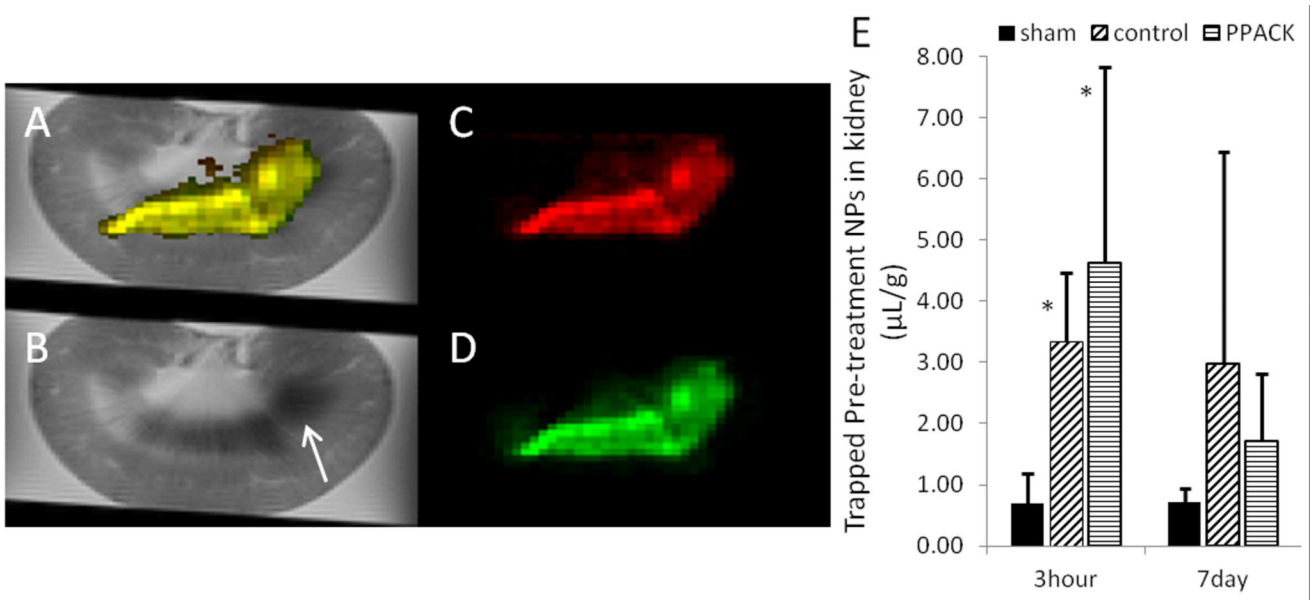

Figure 3.

Ex vivo ^{19}F MRI of trapped NP 3 h after AKI (A–D). Rats were pre-treated with plain PFOB NP and treated after AKI with CE NP. 3h after reperfusion, rats were euthanized and systemically perfused with normal saline to clear circulating NP. Both NP injected before and after AKI are trapped mostly in the medulla region of the kidney. (A) Combined ^{1}H MRI image and ^{19}F MRI images of both pre- and post-treatment NP (yellow). (B) ^{1}H image with arrow showing low signal in damaged medulla. (C) trapped pre-AKI NP (red). (D) trapped post-AKI NP (green). (E) The bar graph illustrates the MR spectroscopy quantification of trapped *pre-AKI* CE NP for rats euthanized 3 h and 7 d after reperfusion. Rats were given a *post-AKI* dose of either PFOB NP or PPACK PFOB NP. Sham injured kidneys exhibited significantly less NP trapped than did AKI groups with either plain NP or PPACK NP post-treatments (p=0.04 by Kruskal-Wallis for the 3 hr groups). Data are presented as means ±SD.. $*P < 0.03$, compared with sham procedure by one-tailed Mann-Whitney test for two independent variables. n=3 for the 3 h sham group; n=4 for the 3 h plain NP group; n=5 for the 3 hr PPACK NP group; n=5 for the 7 d sham group; n=10 for the 7 d plain NP group; n=9 for the 7 d PPACK NP group.

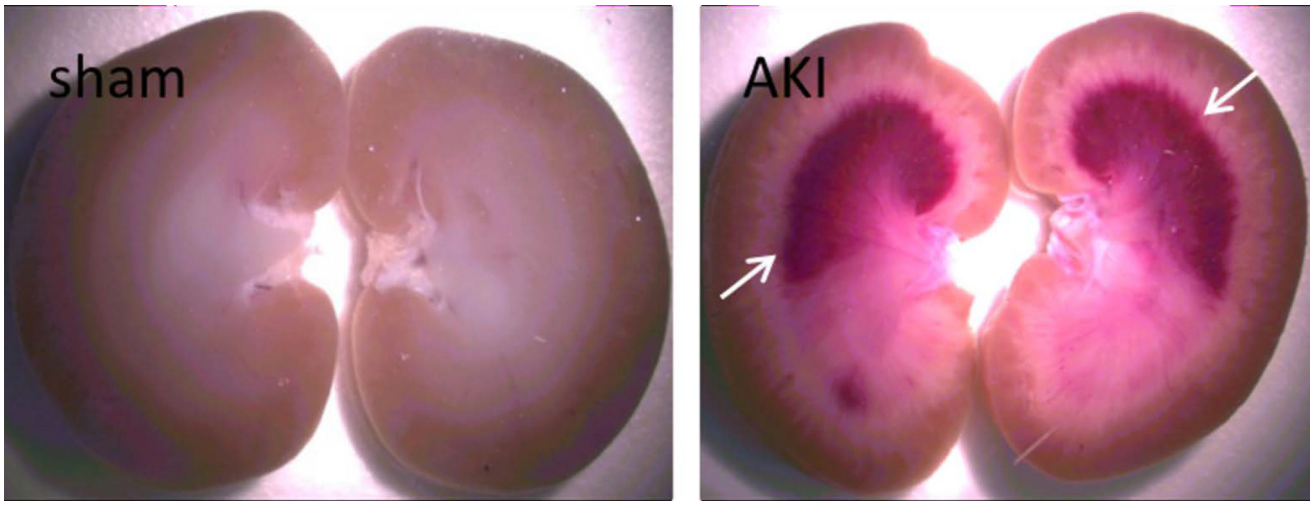

Figure 4.
Image of kidney after AKI showing accumulation of blood in medulla (white arrows).

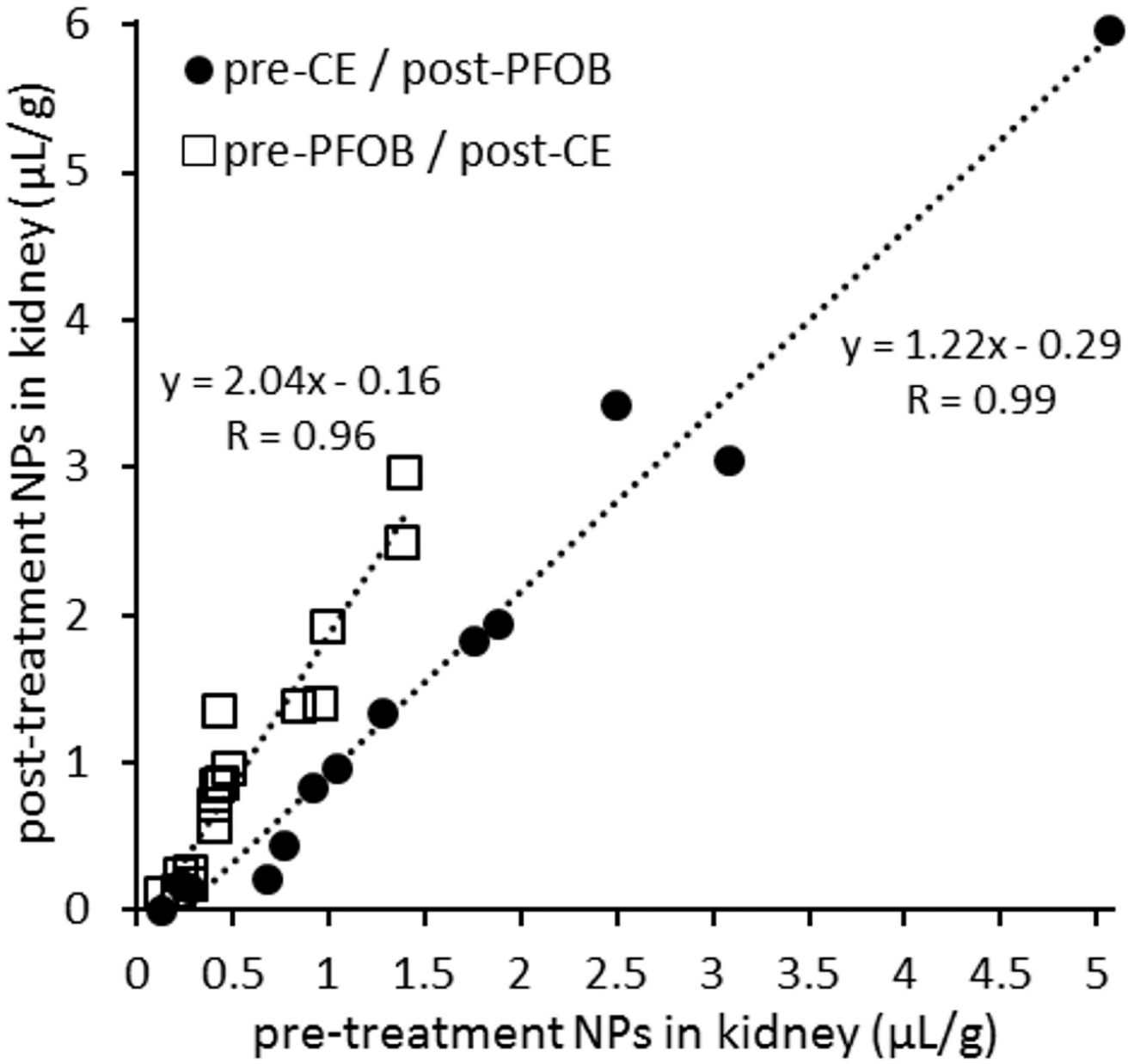

Figure 5.

NP treatments given before and after AKI are linearly correlated. Quantitative ^{19}F MR spectroscopy was used to measure the concentration of trapped NP. Pre-treatment NP were injected 30 min prior to occlusion of the kidney and post-treatment NP were injected during reperfusion of the kidney. The filled circles represent rats with CE-core NP used as the pre-treatment and PFOB-core NP given after AKI. The open squares represent rats given a pre-treatment of PFOB-core NP and CE-core NP after AKI. The two groups were used to confirm that PFC differences did not affect the observations. Both groups are linearly correlated indicating that NP trapping is the same for both particles after reperfusion. NP were given in a 2:1::pre-treatment:post-treatment ratio and this dose ratio was accounted for in this plot.

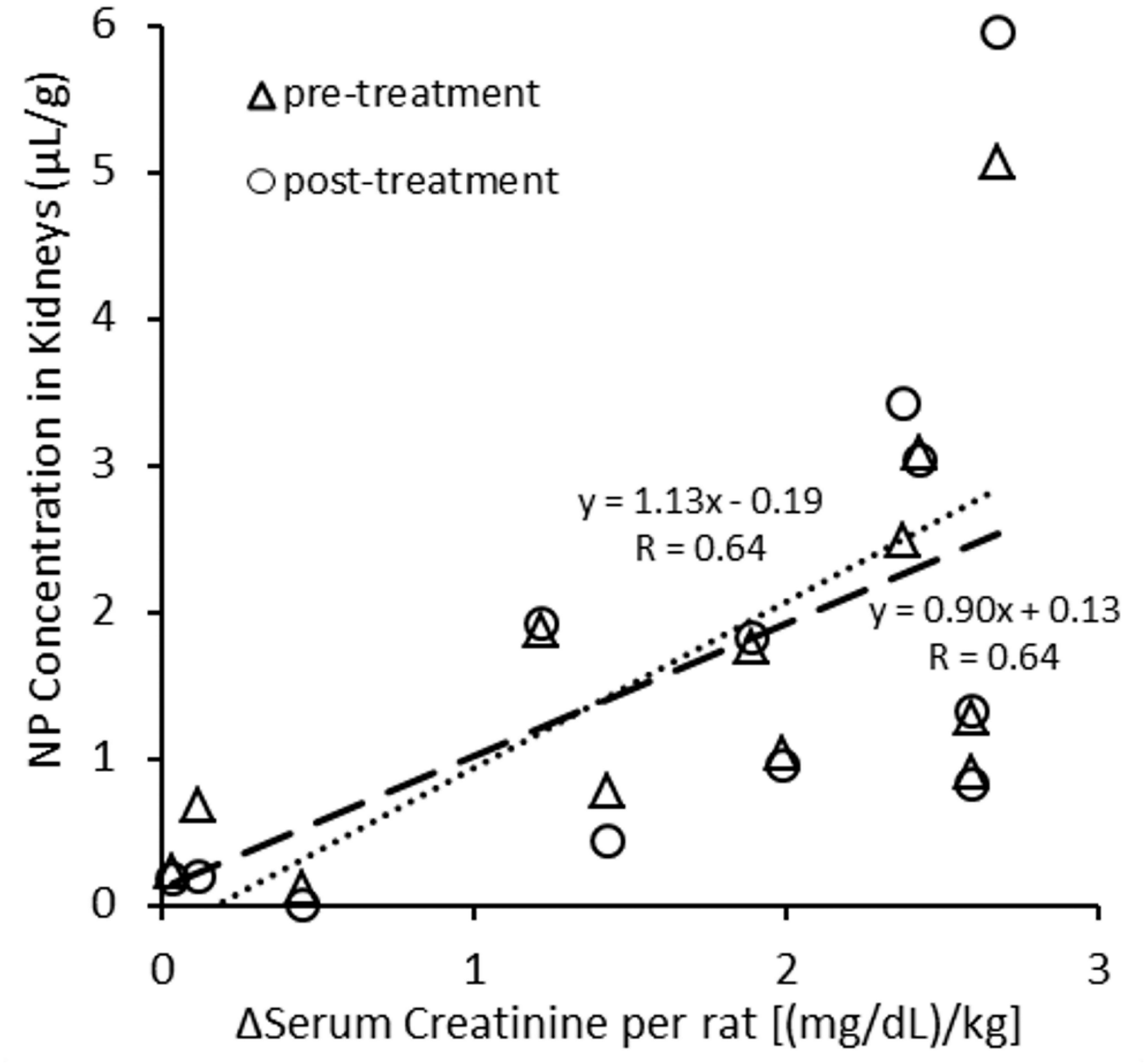

Figure 6.

Trapped NP concentration in kidneys increased as the kidney injury worsened. The change in serum creatinine was measured from pre-AKI to 3 h after AKI. This difference is plotted against the concentration of NP trapped in the kidney as measured by quantitative ^{19}F MR spectroscopy. Pre-treatment NP (CE) are normalized by the dose ratio (2:1).

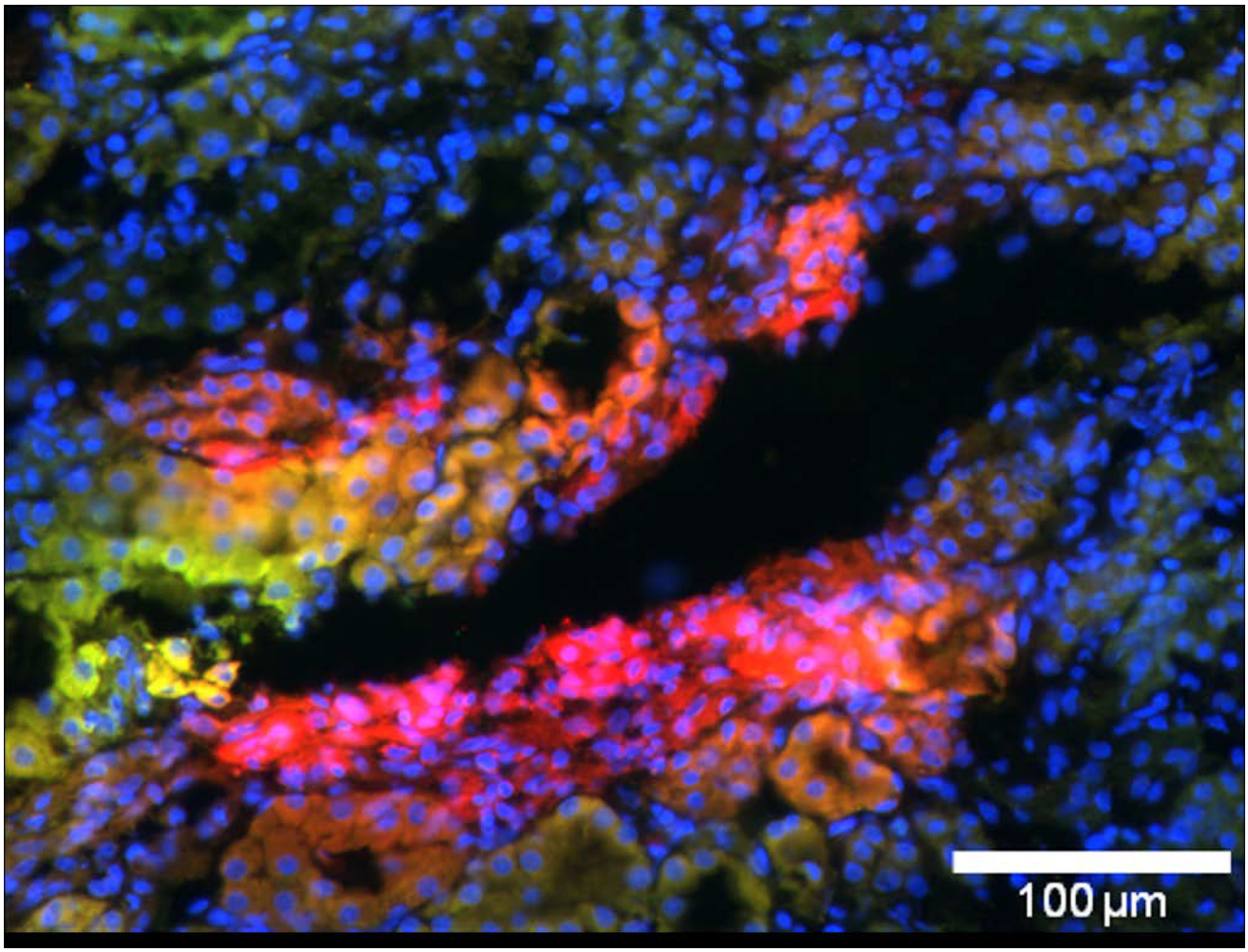

Figure 7.

Example of fluorescent imaging (20×) of NP trapping in the medulla of the kidney that underwent AKI and plain (non targeted) NP treatment. Blue is nuclear staining, green is FITC-labeled NP injected as post-treatment, and red is rhodamine-labeled NP injected as pre-treatment. Red regions indicate areas of pre-treatment NP trapping only. Green regions indicate areas of post-treatment NP trapping only. Yellow-orange regions indicate areas of apparent colocalization. Note that pre-treatment NP (red) are not necessarily co-localized with the post-treatment NP (green).